Extended State Observer-Based Integral Sliding Mode Control for an Underwater Robot with Unknown Disturbances and Uncertain Nonlinearities

Rongxin Cui, *Member, IEEE*, Lepeng Chen, Chenguang Yang, *Senior Member, IEEE*, and Mou Chen, *Member, IEEE*

***Abstract*—This paper develops an novel integral sliding mode controller (ISMC) for a general type of underwater robots based on multiple-input and multiple-output extended-state-observer (MIMO-ESO). The difficulties associated with the unmeasured velocities, unknown disturbances and uncertain hydrodynamics of the robot have been successfully solved in the control design. An adaptive MIMO-ESO is designed not only to estimate the unmeasurable linear and angular velocities, but also to estimate the unknown external disturbances. Then an ISMC is designed using Lyapunov synthesis, and an adaptive gain update algorithm is introduced to estimate the upper bound of the uncertainties. Rigorous theoretical analysis is performed to show that the proposed control method is able to achieve asymptotical tracking performance for the underwater robot. Experimental studies are carried out to validate the effectiveness of the proposed control, and to show that the proposed approach performs better than conventional PD control.**

***Index Terms*—Underwater robot, integral sliding mode controller, extended state observer, underwater vehicle**

I. Introduction

Underwater robots, including autonomous underwater vehicles (AUVs), remote operated vehicles (ROVs) and underwater gliders, have been increasingly utilized to expand the abilities of human in marine resources exploration and marine scientific research. To achieve the full potential benefits provided by underwater robots, high-precision controller for underwater robots is required, such that the quality of the collected data can be guaranteed, and high precision in trajectory tracking or station keeping of the robot can be secured [1]–[6].

In practice, there are a number of technical challenges in the control of an underwater robot, such as the unknown external disturbances and model uncertainties. The unknown disturbances in practical oceanic environments include waves, tides, currents and upward or downward streams. For an ROV, the external force caused by the cable that connects with the depot ship should also be considered. The model uncertainties of an underwater robot are usually caused by the inaccurate hydrodynamic coefficients which are calculated through the computational fluid dynamics (CFD) methods or towing tank experimental data analysis. During the process of performing a task, different attitude of the robot will also cause the variation of the hydrodynamic coefficient.

Several methods, such as adaptive control [1], [7], [8], robust control [9], [10] and disturbance observer-based control [11], [12], have been introduced to address the technical challenges of model uncertainties and unknown external disturbances. In [1], a robust adaptive controller considering the velocity constraints is proposed for an ROV. The model parameters are estimated online and a Barrier Lyapunov function is applied in the Lyapunov synthesis. Finally, the results are validated thought simulation. Since the fuzzy logic systems (FLS) and neural networks (NN) have the ability to approximate nonlinearities, the NN and fuzzy approximation-based adaptive controllers have been widely applied to the plants with model uncertainties and unknown disturbances [7], [8], [13]. In [7], an adaptive controller which combines NN approximation with dynamics surface control is presented for trajectory tracking of an AUV. The computational load is reduced by introducing an NN learning method using minimal number of learning parameters. In [14], considering the unknown parameters, an adaptive fuzzy sliding mode control is presented to steer a low-speed underactuated underwater vehicle and an experiment has justified the method. In [15], the NN-based controller is extended to control the multiple underwater robots and simulation results have been shown. Although the NN and fuzzy-based adaptive controllers have the advantages on the approximation of the uncertainties and disturbances, it is still a challenging task to adjust its learning parameters in real applications.

As an effective tool to suppress disturbances for complex systems, sliding mode control (SMC) has attracted obvious attentions for the control plant with disturbances [10], [16]–[20]. In [21], a novel ESO-based adaptive control has been proposed for power converters to reject the load connected to

Manuscript received October 29, 2016; revised January 26, 2017 and February 18, 2017; accepted March 23, 2017. This work was supported by the National Natural Science Foundation of China (NSFC) under grant 61472325 and grant 51209174. *(Corresponding author: Rongxin Cui.)*

R. Cui and L. Chen are with the School of Marine Science and Technology, Northwestern Polytechnical University, Xi'an 710072, China. (email: r.cui@nwpu.edu.cn).

C. Yang is with the Zienkiewicz Centre for Computational Engineering, Swansea University, SA1 8EN, UK. (email: cyang@theiet.org).

M. Chen is with the College of Automation Engineering, Nanjing University of Aeronautics and Astronautics, Nanjing 210016, China (e-mail: chenmou@nuaa.edu.cn).

the dc-link capacitor and the uncertain parameters. The experiment based on a real power converter prototype validate the control performance. In [9], a sliding mode tracking controller, which uses two sliding surfaces for surge tracking errors and lateral motion tracking errors, is applied to autonomous surface vessels. To address the control technical challenges for the switched stochastic systems, a novel dissipativity-based sliding mode control is proposed in [16]. In [10], integral sliding mode controllers (ISMC) are proposed for trajectory tracking of ROVs. Since the effect of the additional error-integral term, the ISMC has a more accurate trajectory tracking performance than the conventional SMC. To overcome the time-delay for the AUV control, an ISMC is introduced to overcome the problem that data acquisition rate could not be maintained sufficiently [22]. The major shortcoming of SMC is the chattering problem, which not only causes energy losses but also reduces the trajectory tracking smoothness. To reduce the chattering, several methods, such as the high-order sliding-mode controller [23], [24], disturbance compensation method [25], [26], and terminal sliding controller [27] have been proposed. In [25], a free chattering SMC is presented via an adaptive term which continuously compensates for the unknown system dynamics of an ROV. In practice, sometimes, the upper bound of the uncertainties may be large and the SMC without a compensator will cause serious chattering. Therefore, it is necessary to design a compensator for the external disturbance to reduce chattering.

Another approach dealing with the unknown disturbance is to design an observer to estimate the unknown external disturbance of a robot, followed by the control design to compensate for the estimated disturbance. Such disturbance observers include sliding mode observer [11], [28], high-gain observer [29], [30] and extended state observer [12], [31]. In [11], a sliding mode controller based on a sliding mode observer is proposed for a reusable launch vehicle. The observer is presented to estimate the unknown external disturbances and to reduce the control gain. In [29], a high-gain observer-based output feedback motion control that considers the unmodelled dynamics, measurement errors, model parameter variations and unknown external environmental disturbances for observation class ROVs is presented. In [31], a backstepping control based on an extended state observer (ESO) is proposed to handle mismatched disturbance of hydraulic systems. The designed observer estimates not only the model uncertainties but also the unmeasured states. In [12], by using an extended state observer, a backstepping control for a hydraulic system is presented to suppress the large unknown external disturbances. The bandwidth of the observer is chosen in accordance with two conflicting aspects, the maximal load capability and the dynamic performance of system.

In this work, we design an adaptive sliding mode-based controller for a general type of underwater robots, and experiment is carried on a test bed for underwater object grasping. Onboard sensors, including a depth sensor and an inertial measurement unit (IMU), are equipped to measure the depth and attitude of the robot. The position of the underwater robot is measured by an external vision positioning system (VPS) and some white lightings are equipped on the robot which can be captured by the VPS to calculate the position of the robot. In such a case, there is no direct measurement of velocity of the robot. Then output feedback is required for our work as the direct differential of the position information may degrade the control performance. In such case, observes are always used to estimate the unmeasured states of the robot [5], [32]. A local recurrent NN-based adaptive terminal sliding mode state observer is presented to estimate the unmeasured velocity of an ROV in [5], which considers the uncertain dynamic model, the unmeasured states and inaccurate thrust model. In [33], an NN-based adaptive observer is presented to address the problem of estimating the unavailable measurements of underwater vehicles' velocities. In [34], a terminal sliding mode observer of an AUV is introduced to estimate the velocity, and the estimation error is guaranteed to converge to zero in a finite time. In [35], an adaptive backstepping control is introduced for human upper limbs in the presence of disturbances, unmodeled dynamics and uncertainties. In [36], an output feedback tracking controller is designed to address the problem of steering a quadrotor with unknown disturbances and model uncertainties. The unmeasurable linear and angular velocities are estimated by a series of nonmodel-based filters. In [37], an attitude and speed controller is designed based on an adaptive second order SMC for an unmanned aerial vehicle (UAV) and an extended observer is applied to estimate the unmeasured states and unknown external disturbances. In [38], a high gain observer is implemented to estimate the full states of the electro-hydraulic system. It is noted that in the literature mentioned above, controllers designed for underwater robots in [1], [3], [4], [7], [8], [15], [17], [25], [27] are verified by simulations, and other controllers in [6], [10], [14], [22], [23] are verified by experiments.

In this paper, a disturbance compensation approach is utilized to eliminate the chattering based on MIMO-ESO with a simple structure. Motivated by the ESO model [31] and the high-gain observer [38], a MIMO-ESO is proposed to estimate the unknown disturbances and the unmeasured states. The bounds of the uncertainties are also estimated using the adaptive control technique. The Lyapunov analysis is involved to design the final control law. The proposed controller in this paper includes two parts, namely the equivalent controller and the switch controller, which guarantees the trajectory tracking error converge to zero theoretically. The proposed controller is successfully implemented on an underwater robot propelled by six thrusters. The main contributions can be summarized as follows.

1) A novel adaptive MIMO-ESO is developed to estimate the unmeasured velocity and the unknown external disturbances of the underwater robot.
2) Based on Lyapunov analysis, an adaptive MIMO-ESO based ISMC is designed to ensure that the trajectory tracking error converge to zero.
3) Comparative studies with the conventional PD control are carried out experimentally on an underwater robot to demonstrate the superior performance of the proposed control.

The remainder of this paper is organized as follows. Section

II presents the robot model and formulates the problem. In Section III, the adaptive MIMO-ESO is derived to estimate the unknown disturbances and the unmeasured velocities. In section IV, the integral sliding mode controller is proposed. Experimental results are shown in Section V, followed by the conclusion of this work in Section VI.

II. Problem Formulation

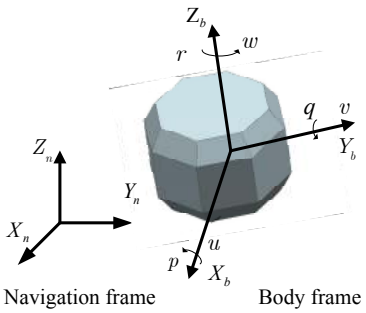

Fig. 1. Navigation and body frames of an underwater robot.

Following the underwater modeling methods in [39], two frames, namely, the navigation frame and the body frame are defined as shown in Fig. 1. The linear velocity $\nu_1 = [u, v, w]^\top$ and the angular velocity $\nu_2 = [p, q, r]^\top$ are defined in the body frame. The position $\eta_1 = [x, y, z]^\top$ and orientations $\eta_2 = [\phi, \theta, \psi]^\top$ are defined in the navigation frame. The nonlinear dynamics of the robot with respect to the body frame is described as

$$M\dot{\nu} + C(\nu)\nu + D(\nu)\nu + G(\eta) = F + d \tag{1}$$

where $\nu = [\nu_1^\top, \nu_2^\top]^\top$, $\eta = [\eta_1^\top, \eta_2^\top]^\top$, d is the unknown external disturbance, and F is the force and moment acting on the robot. Detailed definition of other symbols can be found in [39].

In practical applications, we may not be able to obtain the accurate hydrodynamics coefficients used in the model, thus we divide the matrices in (1) into two parts, namely the nominal value part and the bias part that describes the difference between the real value and the nominal value, i.e., $M = M^* + \Delta M$, $G(\eta) = G^*(\eta) + \Delta G(\eta)$, $C(\nu) = C^*(\nu) + \Delta C(\nu)$, and $D(\nu) = D^*(\nu) + \Delta D(\nu)$, where $(\cdot)^*$ denotes the nominal value that can be obtained from the CFD computation or the tower tank experiment analysis. These nominal values are available for control design. $\Delta(\cdot)$ denotes the difference between the real value and the nominal value. In this work, we consider an underwater robot that equips six thrusters. The moment and force acting on the robot by the thrusters is defined as $F = LU$, where U is a vector describing the force generated by the thrusters, L is the force allocation matrix which is related to the center of buoyancy (COB) and the center of gravity (COG) of the robot.

Now, the model of the underwater robot studied in this work can be written as

$$M^*\dot{\nu} + C^*(\nu)\nu + D^*(\nu)\nu + G^*(\eta) = LU + d_{sum}(\eta, \nu) \tag{2}$$

where $d_{sum}(\eta, \nu)$ is the lumped disturbance, which includes uncertain hydrodynamics and unknown external disturbance. It is defined as $d_{sum}(\eta, \nu) = d + d_{un}$, where

$$d_{un} = -\Delta M\dot{\nu} - \Delta G(\eta) - \Delta C(\nu)\nu - \Delta D(\nu)\nu \tag{3}$$

The kinematics of the robot is described as

$$\dot{\eta} = J(\eta)\nu \tag{4}$$

where $J(\eta)$ is the transformation matrix that relates between speeds in the body and navigation frames. We assume that during the motion of the underwater robot, $\theta \neq 90^\circ$, i.e., J is invertible. Thus, the model of the robot in the navigation frame can be written as

$$\ddot{\eta} + C_\eta(\eta, \nu)\dot{\eta} + D_\eta(\eta, \nu)\dot{\eta} + G_\eta(\eta) = M_\eta LU + H \tag{5}$$

where $C_\eta = JM^{*-1}C^*J^{-1} - \dot{J}J^{-1}$, $D_\eta = JM^{*-1}D^*J^{-1}$, $G_\eta = JM^{*-1}G^*$, $M_\eta = JM^{*-1}$, $H = H_d + H_{un} = M_\eta d_{sum}$ $H_d = M_\eta d$, $H_{un} = M_\eta d_{un}$.

Assumption 1: The unknown external disturbance term $d(t)$ and the first time derivative $\dot{d}(t)$ are bounded. Moveover, $H_d(t)$ and $\dot{H}_d(t)$ are bounded as well. The upper bound of $\dot{H}_d(t)$ is unknown for the control design.

The uncertain items in the robot's model, ΔM, ΔG, ΔC and ΔD are related to the states of the robot. In practice, we can also have the following assumption.

Assumption 2: ΔM, ΔG, ΔC and ΔD are bounded. Then, we assume that d_{un} and $H_{un}(t)$ are also bounded, satisfying $\|H_{un}(t)\| \leq \rho_1 \in \mathbb{R}^+$, where ρ_1 is the unknown upper bound and $\|\cdot\|$ is the Euclidean norm.

In this work, the underwater robot is equipped with an IMU which is used to measure the orientations of η_2. Position of the robot η_1 is measured by an external VPS. There is no sensor available to measure the velocity of the robot directly. Thus, in this work, we design a proper control input, $U(t)$, using the IMU, VPS measurements, to control the trajectory of the underwater robot $\eta(t)$ following the reference trajectory $\eta_r(t)$, i.e., the trajectory tracking error of the robot $\lim_{t\to\infty} e(t) = \lim_{t\to\infty}(\eta(t) - \eta_r(t)) = 0$.

III. Adaptive Extended-state-observer design

In this section, motivated by the adaptive sliding mode observer [40] and the ESO [31], we design an adaptive multiple-input and multiple-output extend-state-observer (MIMO-ESO). Beside the velocity estimation, the unknown external disturbance H_d is estimated simultaneously.

A. Extended-state-observer Design

The extended state vector X can be defined as $X = [x_1^\top, x_2^\top, x_3^\top]^\top = [\eta^\top, \dot{\eta}^\top, H_d^\top]^\top$. The unknown external disturbance H_d is defined as an extended state. According to (5), we have

$$\begin{aligned} \dot{X} &= AX + f(X) + BU(t) + \chi \\ Y &= CX \end{aligned} \tag{6}$$

where

$$A = \begin{bmatrix} 0_{6\times6} & I_{6\times6} & 0_{6\times6} \\ 0_{6\times6} & 0_{6\times6} & I_{6\times6} \\ 0_{6\times6} & 0_{6\times6} & 0_{6\times6} \end{bmatrix}, B = \begin{bmatrix} 0_{6\times6} \\ M_\eta L \\ 0_{6\times6} \end{bmatrix} \tag{7}$$

$$f(X)=\begin{bmatrix}0_{6\times1}\\ \varphi(x_1,x_2)\\ 0_{6\times1}\end{bmatrix},\chi=\begin{bmatrix}0_{6\times1}\\ H_{un}\\ \dot{H}_d\end{bmatrix},C=[I_{6\times6},0_{6\times12}] \quad (8)$$

$$\varphi(x_1,x_2)=-C_\eta(\eta,\nu)\dot{\eta}-D_\eta(\eta,\nu)\dot{\eta}-G_\eta(\eta) \quad (9)$$

The adaptive MIMO-ESO is presented as

$$\begin{aligned}\dot{\hat{X}}&=A\hat{X}+f(\hat{X})+BU(t)-\kappa(\hat{x}_1-x_1)-Q\varpi\\ \hat{Y}&=C\hat{X}\end{aligned} \quad (10)$$

where $\hat{X}$ is the estimation of X, the gain κ is designed as

$$\kappa=[3w_0I_{6\times6},3w_0^2I_{6\times6},w_0^3I_{6\times6}]^\top\in\mathbb{R}^{18\times6} \quad (11)$$

where w_0 is the bandwidth of the ESO.

$$Q=\begin{bmatrix}I_{6\times6}&0_{6\times6}&0_{6\times6}\\ 0_{6\times6}&w_0I_{6\times6}&0_{6\times6}\\ 0_{6\times6}&0_{6\times6}&w_0^2I_{6\times6}\end{bmatrix},f(\hat{X})=\begin{bmatrix}0_{6\times1}\\ \hat{\varphi}(\hat{x}_1,\hat{x}_2)\\ 0_{6\times1}\end{bmatrix} \quad (12)$$

$$\varpi(\tilde{Y},\hat{\rho}_2)=\begin{cases}\frac{P^{-1}C^\top\tilde{Y}\hat{\rho}_2-c_1P^{-1}C^\top\tilde{Y}\dot{h}_1(t)\hat{\rho}_2^2/\|\tilde{Y}\|}{\|\tilde{Y}\|-c_1\dot{h}_1(t)\hat{\rho}_2}, & if\quad \|\tilde{Y}\|\neq0\\ 0_{18\times1}, & if\quad \|\tilde{Y}\|=0\end{cases} \quad (13)$$

where $\tilde{Y}=\hat{Y}-Y$, c_1 is a positive constant, $\hat{\rho}_2$ is positive and will be defined later, $\dot{h}_1(t)$ is designed to satisfy $\sup_{t\in R^+}\dot{h}_1(t)<0$. Those parameters ensure the positive definiteness of $\|\tilde{Y}\|-c_1\dot{h}_1(t)\hat{\rho}_2$.

The uncertain and first time derivative of external disturbance parts are assumed to satisfy a matching condition [41]

$$-G_3\dot{H}_d/w_0^2-G_2H_{un}/w_0=P^{-1}C^\top\rho_t(t) \quad (14)$$

Remark 1: In this work, both unmeasured velocity and the external disturbances are considered in the control design. The bounds of the disturbances are assumed to be unavailable for the control design, thus an ESO is introduced to estimate the unmeasured velocity and the disturbance. Similar to works in [41], the matching condition (14) is assumed to be existed that facilitates subsequent stability proof. For the systems which don't satisfy the matching condition, there have been several works that relax the matching condition, such as [42] in which an additional observer is introduced to observe the unknown inputs. This inspires us that one of the future research directions lies in the relaxing of such matching condition.

According to Assumption (1) and (2), we know that $\dot{H}_d$ and H_{un} are bounded. From (14), $\rho_t(t)$ is bounded and satisfies $\|\rho_t(t)\|\leq\rho_2\in\mathbb{R}^+$, where the upper bound ρ_2 is unknown. The update law of its estimation $\hat{\rho}_2$, is designed as

$$\dot{\hat{\rho}}_2=\gamma_2\|\tilde{Y}\| \quad (15)$$

where γ_2 is a positive constants and we define $\hat{\rho}_2(0)=0$.

The estimation error is defined as $\tilde{X}=\hat{X}-X=[\tilde{x}_1^\top,\tilde{x}_2^\top,\tilde{x}_3^\top]^\top$. The scaled estimation errors are defined as $\varepsilon_i=\tilde{x}_i/w_0^{i-1}\in\mathbb{R}^6,i=1,2,3$. Then, subtracting (6) from (10), we can describe the observer scaled estimation error as

$$\begin{aligned}\dot{\varepsilon}=&-w_0A_\varepsilon\varepsilon+Q^{-1}\tilde{f}-G_3\dot{H}_d/w_0^2\\ &-G_2H_{un}/w_0-\varpi(\tilde{Y},\hat{\rho}_2)\\ =&-w_0A_\varepsilon\varepsilon+Q^{-1}\tilde{f}+P^{-1}C^\top\rho_t(t)-\varpi(\tilde{Y},\hat{\rho}_2)\end{aligned} \quad (16)$$

where $\varepsilon=[\varepsilon_1^\top,\varepsilon_2^\top,\varepsilon_3^\top]^\top$ with $\varepsilon_i=[\varepsilon_{i1},\cdots,\varepsilon_{i6}]^\top$, $G_3=[0_{12\times6},I_{6\times6}]^\top$, $G_2=[0_{6\times6},I_{6\times6},0_{6\times6}]^\top$,

$$A_\varepsilon=\begin{bmatrix}3I_{6\times6}&-I_{6\times6}&0_{6\times6}\\ 3I_{6\times6}&0_{6\times6}&-I_{6\times6}\\ I_{6\times6}&0_{6\times6}&0_{6\times6}\end{bmatrix},\tilde{f}=f(\hat{X})-f(X). \quad (17)$$

It is assumed that all states and the function $\varphi(x_1,x_2)$ are in a compact set. Then, the nonlinear term $\varphi(x_1,x_2)$ is Lipschitz with respect to x_1 and x_2 in the compact set.

Remark 2: Different from the observers which are used to estimate the lumped disturbance that contains the unknown external disturbance and the nonlinear uncertainties in [25], [37], we only estimate the unknown external disturbance. The boundedness of the first time derivative of the lumped disturbance is required for the control design in [25], [37]. In practice, the uncertainty part always includes the velocities of the robot. Then, the time derivative of the uncertainty contains the accelerates which are strongly dependent on the control inputs. The switching control input in the SMC will lead to a large value of the derivative of the uncertainty, which prevents the boundedness assumption of the derivation of uncertainty. In this paper, we regard the unknown external disturbance as an augmented state, thus the assumption is relaxed.

Lemma 1: $\dot{\varepsilon}=-w_0A_\varepsilon\varepsilon+Q^{-1}\tilde{f}+P^{-1}C^\top\rho_t(t)-\varpi$ has a faster convergent rate or a slower divergent rate than $\dot{\varepsilon}=-\beta A_\varepsilon\varepsilon+P^{-1}C^\top\rho_t(t)-\varpi$.

Proof: Since $-A_\varepsilon$ is Hurwitz, there exists a symmetric positive definite matrix P which satisfies

$$A_\varepsilon^TP+PA_\varepsilon=I_{18\times18} \quad (18)$$

Substituting A_ε into (18), we can calculate that

$$P=\begin{bmatrix}I_{6\times6}&-0.5I_{6\times6}&-I_{6\times6}\\ -0.5I_{6\times6}&I_{6\times6}&-0.5I_{6\times6}\\ -I_{6\times6}&-0.5I_{6\times6}&4I_{6\times6}\end{bmatrix} \quad (19)$$

We can obtain that $\|Q^{-1}\tilde{f}\|=\frac{\|\hat{\varphi}-\varphi\|}{w_0}=\frac{\|\tilde{\varphi}\|}{w_0}$ from (8) and (12). According to the assumptions, there are some known constants ζ_1 and ζ_2 that satisfy the following Lipschitz conditions.

$$\|\tilde{\varphi}\|\leq\zeta_1\|\varepsilon_1\|+\zeta_2\|\varepsilon_2\|\leq(\zeta_1+\zeta_2)\|\varepsilon\| \quad (20)$$

Let us choose a Lyapunov function candidate as

$$V_1=\varepsilon^\top P\varepsilon. \quad (21)$$

The time derivative of V_1 can be written as

$$\begin{aligned}\dot{V}_1=&\dot{\varepsilon}^\top P\varepsilon+\varepsilon^\top P\dot{\varepsilon}\\ =&-w_0\varepsilon^\top A_\varepsilon^\top P\varepsilon+(Q^{-1}\tilde{f})^\top P\varepsilon+(P^{-1}C^\top\rho_t)^\top P\varepsilon\\ &-\varpi^\top P\varepsilon-w_0\varepsilon^\top PA_\varepsilon\varepsilon+\varepsilon^\top PQ^{-1}\tilde{f}\\ &+\varepsilon^\top PP^{-1}C^\top\rho_t-\varepsilon^\top P\varpi\end{aligned} \quad (22)$$

Because P is a symmetric positive definite matrix, we have $(Q^{-1}\tilde{f})^\top P\varepsilon=\varepsilon^\top PQ^{-1}\tilde{f}$, $(P^{-1}C^\top\rho_t)^\top P\varepsilon=\varepsilon^\top PP^{-1}C^\top\rho_t$ and $\varpi^\top P\varepsilon=\varepsilon^\top P\varpi$.

$$\begin{aligned}\dot{V}_1=&-w_0\varepsilon^\top(A_\varepsilon^\top P+PA_\varepsilon)\varepsilon+2\varepsilon^\top PQ^{-1}\tilde{f}\\ &+2\varepsilon^\top P\tilde{f}/w_0+2\varepsilon^\top C^\top\rho_t(t)-2\varepsilon^\top P\varpi\end{aligned} \quad (23)$$

Substituting (18) into (23), we have

$$\begin{aligned}\dot{V}_1 =& -w_0\varepsilon^\top\varepsilon + 2\varepsilon^\top PQ^{-1}\tilde{f}/w_0 \\ &+ 2\varepsilon^\top C^\top\rho_t(t) - 2\varepsilon^\top P\varpi \\ \leq& -w_0\|\varepsilon\|^2 + 2\|\varepsilon\|\|P\|\|Q^{-1}\tilde{f}\| \\ &+ 2\varepsilon^\top C^\top\rho_t(t) - 2\varepsilon^\top P\varpi \\ \leq& [-w_0 + c_2(\zeta_1+\zeta_2)/w_0]\,\|\varepsilon\|^2 \\ &+ 2\varepsilon^\top C^\top\rho_t(t) - 2\varepsilon^\top P\varpi\end{aligned} \tag{24}$$

Then, (24) can be rewritten as

$$\dot{V}_1 \leq -\beta\|\varepsilon\|^2 + 2\varepsilon^\top C^\top\rho_t(t) - 2\varepsilon^\top P\varpi \tag{25}$$

where $\beta = w_0 - c_2(\zeta_1+\zeta_2)/w_0 > 0$, c_2 is a positive constant which satisfies $c_2 \geq 2\|P\|$.

According to (25), we can conclude that (16) has a faster convergent rate or a slower divergent rate than $\dot{\varepsilon} = -\beta A_\varepsilon\varepsilon + P^{-1}C^\top\rho_t(t) - \varpi$. This completes the proof. ■

Remark 3: It is not easy to analyze the convergent performance directly through (16). Based on Lemma 1, we only need to analyze the convergent behavior of $\dot{\varepsilon} = -\beta A_\varepsilon\varepsilon + P^{-1}C^\top\rho_t(t) - \varpi$ instead of (16).

IV. Controller Design

To guarantee a satisfied trajectory tracking performance for the underwater robot, an extended state observer-based integral sliding mode controller is proposed in this section.

Before designing the ISMC, let us rewrite the system model as follows.

$$\begin{aligned}\ddot{\eta} =& -C_\eta\dot{\eta} - D_\eta\dot{\eta} - G_\eta + M_\eta LU + H \\ =& -C_\eta\dot{\eta} - D_\eta\dot{\eta} - G_\eta + M_\eta LU + H_{un} + H_d\end{aligned} \tag{26}$$

where $H = M_\eta d_{sum}(\eta,\nu,t)$ is the lumped uncertainty, which consists of three parts, including the external disturbances, the matched uncertainty resulting from the uncertain hydrodynamic coefficients $\Delta C(\nu(t))$ and $\Delta D(\nu(t))$, and the uncertainty of ΔG_η. Our goal is to propose a controller to overcome the problem that the lumped uncertainty $H(t)$ will degrade the control performance.

The integral sliding surface is defined as

$$s(t) = K_p e(t) + K_i\int_0^t e(\tau)d\tau + K_d\hat{\dot{e}}(t) - K_p e(0) - K_d\hat{\dot{e}}(0) \tag{27}$$

where K_p, K_i, and K_d are designed positive definite diagonal matrices.

Similar definitions of the sliding mode surface can be found in [10], [43], [44]. The difference is that we replace the derivative of the tracking error, $\dot{e}(t)$, by its estimation value, $\hat{\dot{e}}(t)$, in this work, since there is no direct measurement of the velocity of the underwater robot. $\hat{\dot{e}}(t)$ in (27) is defined as

$$\hat{\dot{e}}(t) = \hat{\dot{\eta}}(t) - \dot{\eta}_r(t) \tag{28}$$

Employing the derivative on both sides of (27), we have

$$\dot{s}(t) = K_p\hat{\dot{e}}(t) + K_i e(t) + K_d\hat{\ddot{e}}(t) \tag{29}$$

The reaching law can be chosen as

$$\dot{s}(t) = -K_s s - K_{sw}\mathbf{sgn}(s) \tag{30}$$

where K_s and K_{sw} are positive definite diagonal matrices, $\mathbf{sgn}(s) = [\mathrm{sgn}(\mathrm{s}_1),\ldots,\mathrm{sgn}(\mathrm{s}_6)]^\top$.

According to (26), (29) and (30), we can derive

$$\begin{aligned}\dot{s} + K_s s =& K_p\hat{\dot{e}} + K_i e + K_s s + K_d(-\ddot{\eta}_r - C_\eta\hat{\dot{\eta}} \\ &- D_\eta\hat{\dot{\eta}} - G_\eta + M_\eta LU + \hat{H}_d) \\ &- K_d(\hat{H}_d - H_d) + K_d H_{un}\end{aligned} \tag{31}$$

where $\hat{H}_d(t)$ is the estimation of the unknown external disturbance, $\hat{\nu}$ and $\hat{\dot{\eta}}$ are the estimations of ν and $\dot{\eta}$, respectively.

The first part of our control can be designed as

$$\begin{aligned}U_{eq} =& -(K_d M_\eta L)^{-1}(K_p\hat{\dot{e}} + K_i e + K_s s) \\ &+ (M_\eta L)^{-1}[\ddot{\eta}_r + C_\eta(\eta,\hat{\nu})\hat{\dot{\eta}} \\ &+ D_\eta(\eta,\hat{\nu})\hat{\dot{\eta}} + G_\eta - \hat{H}_d]\end{aligned} \tag{32}$$

Substituting U_{eq} into U in (31), we have

$$\begin{aligned}\dot{s} =& -K_s s - K_d(\hat{H}_d - H_d) + K_d H_{un} \\ =& -K_s s - K_d\tilde{H}_d + K_d H_{un}\end{aligned} \tag{33}$$

where $\tilde{H}_d = \hat{H}_d - H_d$.

We design the switching control as

$$\begin{aligned}U_{sw} =& \\ &-\left[(K_d M_\eta L)^{-1}K_{sw} + \lambda_{\max}(K_d)\hat{\rho}_1(K_d M_\eta L)^{-1}\right]\mathbf{sgn}(s)\end{aligned} \tag{34}$$

where $\hat{\rho}_1$ is the estimation of ρ_1 and $\tilde{\rho}_1 = \hat{\rho}_1 - \rho_1$ is the estimation error.

The gain update law of $\hat{\rho}_1$ is designed as follows

$$\dot{\hat{\rho}}_1 = \gamma_1\lambda_{\max}(K_d)\|s\| \tag{35}$$

where γ_1 is designed positive constant.

Combining (32) and (34), the complete control law can be described as follows

$$\begin{aligned}U =& U_{eq} + U_{sw} \\ =& -(K_d M_\eta L)^{-1}(K_p\hat{\dot{e}} + K_i e + K_s s) \\ &+ (M_\eta L)^{-1}[\ddot{\eta}_r + C_\eta(\eta,\hat{\nu})\hat{\dot{\eta}} + D_\eta(\eta,\hat{\nu})\hat{\dot{\eta}} + G_\eta \\ &- \hat{H}_d] - (K_d M_\eta L)^{-1}K_{sw}\mathbf{sgn}(s) \\ &- \lambda_{\max}(K_d)\hat{\rho}_1\,(K_d M_\eta L)^{-1}\,\mathbf{sgn}(s)\end{aligned} \tag{36}$$

where $\lambda_{\max}(\cdot)$ and $\lambda_{\min}(\cdot)$ are the maximum and minimum eigenvalues of a matrix, respectively.

Lemma 2: [45] If a signal has a bounded derivative and is square integrable, the signal can converge to zero asymptotically.

Theorem 1: Consider the uncertain system (6) satisfying Assumptions 1 and 2, with the designed ESO (10), the integral sliding mode controller (36), and the gain adaption law (35). The system tracking error and external disturbance estimation error will converge to zero if the parameters β, w_0, K_d, K_s, and K_{sw} satisfy the following conditions: $\beta > w_0^4\lambda_{\max}(K_d)$, $\lambda_{\min}(K_s) > \frac{\lambda_{\max}(K_d)}{2}$ and $\lambda_{\min}(K_{sw}) > 0$.

Proof: Now, we define a Lyapunov function candidate

$$V = \frac{1}{2}V_1 + \frac{1}{2}s^\top s + \frac{1}{2\gamma_1}\tilde{\rho}_1^2 + \frac{1}{2\gamma_2}\tilde{\rho}_2^2 \tag{37}$$

where V_1 is defined in (21).

According to Lemma 1, we have

$$\begin{aligned}\dot{V} \leq & -\frac{\beta}{2}(\varepsilon_1^\top\varepsilon_1+\varepsilon_2^\top\varepsilon_2+\varepsilon_3^\top\varepsilon_3)+\varepsilon^\top C^\top\rho_t(t)\\ & -\varepsilon^\top P\varpi+s^\top\dot{s}+\frac{1}{\gamma_1}\tilde{\rho}_1\dot{\hat{\rho}}_1+\frac{1}{\gamma_2}\tilde{\rho}_2\dot{\hat{\rho}}_2\end{aligned} \tag{38}$$

Substituting (13) and (15) into (27), we have

$$\begin{aligned}\dot{V} \leq & -\beta\varepsilon^\top\varepsilon/2+s^\top\dot{s}+\tilde{\rho}_1\dot{\hat{\rho}}_1/\gamma_1\\ & +\|\tilde{Y}\|\rho_2-\varepsilon^\top P\varpi+\|\tilde{Y}\|\tilde{\rho}_2\\ \leq & -\beta\varepsilon^\top\varepsilon/2+s^\top\dot{s}+\tilde{\rho}_1\dot{\hat{\rho}}_1/\gamma_1+\|\tilde{Y}\|\hat{\rho}_2\\ & -\frac{\|\tilde{Y}\|^2\hat{\rho}_2-c_1\|\tilde{Y}\|^2\dot{h}_1\hat{\rho}_2^2/\|\tilde{Y}\|}{\|\tilde{Y}\|-c_1\dot{h}_1\hat{\rho}_2}\\ = & -\beta\varepsilon^\top\varepsilon/2+s^\top\dot{s}+\tilde{\rho}_1\dot{\hat{\rho}}_1/\gamma_1\end{aligned} \tag{39}$$

Substituting (36) into (31), we have

$$\begin{aligned}\dot{s} = & -K_s s-\lambda_{\max}(K_d)\hat{\rho}_1\mathbf{sgn}(s)-K_{sw}\mathbf{sgn}(s)\\ & -K_d\tilde{H}_d+K_dH_{un}\end{aligned} \tag{40}$$

Substituting (35) and (40) into (39), we see that the derivative of V can be described as

$$\begin{aligned}\dot{V} \leq & -\frac{\beta}{2}\varepsilon^\top\varepsilon-s^\top K_s s\\ & -s^\top K_{sw}\mathbf{sgn}(s)-\lambda_{\max}(K_d)\hat{\rho}_1 s^\top\mathbf{sgn}(s)\\ & -s^\top K_d\tilde{H}_d+s^\top K_dH_{un}+\lambda_{\max}(K_d)\tilde{\rho}_1\|s\|\end{aligned} \tag{41}$$

where $\tilde{H}_d = w_0^2\varepsilon_3$, $-s^\top K_d\tilde{H}_d \leq \lambda_{\max}(K_d)(\|s\|^2+w_0^4\|\varepsilon_3\|^2)/2$, $-s^\top K_s s \leq -\lambda_{\min}(K_s)\|s\|^2/2$, $s^\top K_dH_{un} \leq \lambda_{\max}(K_d)\|H_{un}\|\|s\|$.

Then, we have

$$\begin{aligned}\dot{V} \leq & -\frac{\beta}{2}\varepsilon^\top\varepsilon-\lambda_{\min}(K_s)\|s\|^2+\frac{\lambda_{\max}(K_d)}{2}(\|s\|^2\\ & +w_0^4\|\varepsilon_3\|^2)+\lambda_{\max}(K_d)\|H_{un}\|\|s\|+\lambda_{\max}(K_d)\tilde{\rho}_1\|s\|\\ & -\lambda_{\max}(K_d)\hat{\rho}_1\|s\|-s^\top K_{sw}\mathbf{sgn}(s)\\ \leq & -\frac{\beta}{2}\|\varepsilon_1\|^2-\frac{\beta}{2}\|\varepsilon_2\|^2-\left[\frac{\beta}{2}-\frac{1}{2}w_0^4\lambda_{\max}(K_d)\right]\|\varepsilon_3\|^2\\ & -\left[\lambda_{\min}(K_s)-\frac{1}{2}\lambda_{\max}(K_d)\right]\|s\|^2\\ & -\lambda_{\max}(K_d)(\rho_1-\|H_{un}\|)\|s\|-\lambda_{\min}(K_{sw})\|s\|\\ \leq & -\xi^\top\Lambda\xi-[\lambda_{\min}(K_{sw})+\lambda_{\max}(K_d)(\rho_1-\|H_{un}\|)]\|s\|\end{aligned} \tag{42}$$

where $\xi = [\varepsilon^\top, s^\top]^\top$, $\Lambda = \begin{bmatrix}\Lambda_1 & 0_{12\times6} & 0_{12\times6}\\ 0_{6\times6} & \Lambda_2 & 0_{6\times6}\\ 0_{6\times6} & 0_{6\times6} & \Lambda_3\end{bmatrix}$, $\Lambda_1 = \frac{\beta}{2}I_{12\times12}$, $\Lambda_2 = \left[\frac{\beta}{2}-\frac{1}{2}w_0^4\lambda_{\max}(K_d)\right]I_{6\times6}$, $\Lambda_3 = \left[\lambda_{\min}(K_s)-\frac{1}{2}\lambda_{\max}(K_d)\right]I_{6\times6}$.

Based on Assumption 2, we have $\rho_1-\|H_{un}\| \geq 0$. Because the parameters β, w_0, K_s and K_{sw} satisfy related conditions mentioned in Theorem 1, we know that $\lambda_{\min}(K_{sw})>0$ and $\lambda_{\min}(\Lambda)>0$.

Inequation (42) implies that $\dot{V}<0$ for $\xi\neq0$, and the signals s, ε, $\tilde{\rho}_1$ and $\tilde{\rho}_2$ are bounded. Based on (42), we have $\dot{V} \leq -\xi^\top\Lambda\xi$. Then, we have $\lim_{t\to\infty}\int_0^t(\xi^\top\Lambda\xi)d\tau \leq V(0)-V(\infty)$. Because $V(0)$ and $V(\infty)$ are bounded, s and ε are square integrable. According to (40) and the boundedness of s, $\hat{\rho}_1$, $\dot{H}_d$ and H_{un}, we can conclude that $\dot{s}$ is bounded.

From (12), we know that $\|\tilde{f}\| = \|\tilde{\varphi}\|$. Further, we have $\tilde{f}$ is bounded according to (14). The boundedness of $\dot{H}_d$ and H_{un} implies that $\rho_t(t)$ is bounded from (14). Because ε, $\hat{\rho}_2$ and $\dot{h}(t)$ are bounded, from (13), we can obtain ϖ is bounded. Then, $\dot{\varepsilon}$ is bounded from (16). The boundedness of $\dot{s}$ and $\dot{\varepsilon}$ implies that $\dot{\xi}$ is bounded. According to Lemma 2, we have $\lim_{t\to\infty}\xi(t)=0$, i.e., $\lim_{t\to\infty}s(t)=0$ and $\lim_{t\to\infty}\varepsilon(t)=0$.

Substituting $\hat{e} = \hat{\dot{\eta}}-\dot{\eta}$ into (27), we have

$$K_pe(t)+K_i\int_0^t e(\tau)d\tau+K_d\dot{e}(t)+K_de(0) = z(t) \tag{43}$$

where $z(t) = [z_1(t),\cdots,z_6(t)]^\top$ satisfies

$$z(t) = s(t)-w_0K_d\varepsilon_2(t)+K_pe(0)+K_d\hat{\dot{e}}(0)+K_de(0) \tag{44}$$

Because K_p, K_i and K_d are positive definite diagonal matrices, we have

$$\begin{aligned}z_i(t) = & K_{pi}e_i(t)+K_{ii}\int_0^t e_i(\tau)d\tau+K_{di}\dot{e}_i(t)\\ & +K_{di}e(0),\ \ i=1,\ldots,6\end{aligned} \tag{45}$$

where $z_i(t)$ is the ith element of $z(t)$.

Then, take Laplace transform of (45), we have

$$\frac{e_i(p)}{z_i(p)} = \frac{p}{K_{di}p^2+K_{pi}p+K_{ii}} \tag{46}$$

where p is the Laplace transform operator, $e_i(p)$ and $z_i(p)$ are the Laplace transforms of $e_i(t)$ and $z_i(t)$, respectively.

Using the final value theorem of Laplace transform, we have

$$e(\infty) = \lim_{p\to0}\frac{p^2z_i(p)}{K_{di}p^2+K_{pi}p+K_{ii}} \tag{47}$$

Let $p = \mathrm{Re}(p)+i\mathrm{Im}(p) = p_r+ip_i$. Since the initial error $e(0)$ and $\hat{\dot{e}}(0)$ are bounded, and $\varepsilon_2(t)$ is bounded, from (44), $z_i(t)$ is bounded. $z_i(t)$ can converge to $K_pe(0)+K_d\hat{\dot{e}}(0)+K_de(0)$ as time goes to infinity. Then, we have $|z_i(t)| \leq z_{i\max}<\infty$. The Laplace transform of $z_i(t)$ satisfies

$$\begin{aligned}|z_i(t)| = & \left|\int_0^\infty e^{-p\tau}z_i(\tau)d\tau\right| \leq \int_0^\infty|e^{-p\tau}z_i(\tau)|d\tau\\ \leq & z_{i\max}\int_0^\infty|e^{-p\tau}|dt = z_{i\max}\int_0^\infty|e^{-(p_r+ip_i)\tau}|d\tau\\ \leq & z_{i\max}\int_0^\infty|e^{-p_r\tau}||e^{-ip_i\tau}|d\tau\\ \leq & z_{i\max}\int_0^\infty|e^{-p_r\tau}||\cos(-p_i\tau)+i\sin(-p_i\tau)|d\tau\\ = & \frac{z_{i\max}}{p_r}\end{aligned} \tag{48}$$

Then, we have

$$\begin{aligned}\lim_{p\to0}|p^2z_i(p)| \leq & \lim_{p_r\to0,p_i\to0}\left(|p_r+ip_i|^2\left|\frac{z_{i\max}}{p_r}\right|\right)\\ \leq & \lim_{p_r\to0}\left(p_r^2\left|\frac{z_{i\max}}{p_r}\right|\right)=0\end{aligned} \tag{49}$$

Hence, it can be induced from (49) that $\lim_{p\to 0} p^2 z_i(p) = 0$. Then,

$$e_i(\infty) = \lim_{p\to 0} \frac{p^2 z_i(p)}{K_{di}p^2 + K_{pi}p + K_{ii}} = 0 \qquad (50)$$

The system given by (45) and (46) is stable if the parameters K_{di}, K_{pi} and K_{ii} are chosen as positive constants to satisfy Hurwitz stability criterion. According to (47) and (50), it can be concluded that $\lim_{t\to\infty} e(t) = 0$. This completes the proof. ■

Remark 4: Given that many parameters need to be chosen for the control design, we provide a guidance on choosing the control parameters. The parameters can be divided into three parts as follows. (i) K_p, K_d and K_i in (27) relate to the the dynamic convergent performance of trajectory tracking error, which should be chosen as positive definite matrices to satisfy Hurwitz stability criterion. (ii) K_{sw} and K_s in (30) are associated with the control stability and the rate of reaching the sliding mode surface. K_{sw} is a positive definite matrix satisfying $\lambda_{\min}(K_s) > \frac{\lambda_{\max}(K_d)}{2}$ in order to guarantee the positive definite property of matrix Λ in (42). Besides, since large K_{sw} may lead to chattering problem, it is expected to decrease $\min K_{sw}$ as small as possible. K_s can effect the rate of reaching the sliding mode surface. (iii) γ_1, γ_2, c_1 are the parameters for the ESO. w_0 is an important parameter for the observer. If w_0 is selected very large, the estimation of the states can vibrate sharply in the beginning; this it is harmful to the control performance. A small w_0 leads to a slow converge rate of the estimation error. γ_1 and γ_2 have influences on the convergence rates of $\tilde{\rho}_1$ and $\tilde{\rho}_2$, respectively. These two parameters can be chosen empirically.

V. Experiment Studies

This section describes the experiment studies we have performed to verify the developed controller via an underwater robot propelled by six thrusters. The designed controller is compared with the conventional PD controller during experiment study.

A. Experiment Setup

As shown in Fig. 2(a), the underwater robot used in the experiment measures $574\times574\times454.5mm$ and weights 60kg. It is equipped with six separate thrusts, $U = [U_1, \ldots, U_6]^\top$, in which two thrusts (U_1, U_5) are used for surge motion, two thrusts (U_2, U_4) are used for sway motion and two thrusts (U_3, U_6) are used for heave motion. The thrusters can provide the thrust $U_i \in [-20, 20]N$, $i = 1, \cdots, 6$. An IMU is used to measure the orientations of the robot in the body frame and the measurement accuracy is $0.4°$. A VPS, which is equipped with two cameras next to the pool and four white light sources on the robot, is applied to measure positions of the underwater robot whose white lights are all turned on during the experiment for the position capturing by the VPS as presented in Fig. 2(b).

The underwater robot includes an internal computer system which connects to external computer via fiber-optic communication. The internal computer system is composed by PC104 module. Both internal and external computer system use Windows XP operating systems. The internal computer system receives the IMU data and transmits it to the external computer. The external computer receives this information and the position information from the VPS, and calculates the control input for each thruster. Then, the control signals are transmitted to the internal computer which connects to six thrusters. The signal flow of the control system is presented in Fig. 3.

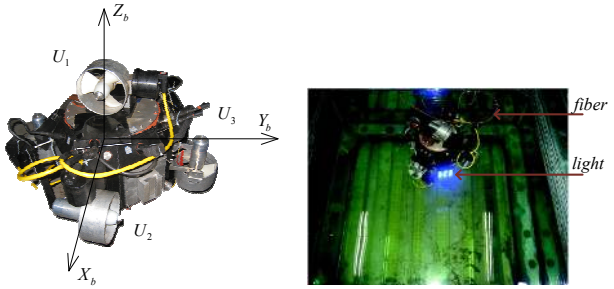

(a) (b)

Fig. 2. (a) The underwater robot used in the experiment. (b) The underwater robot in the pool.

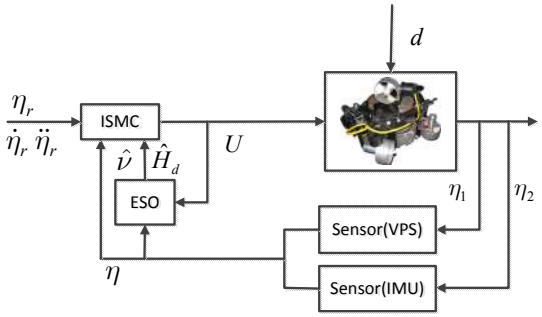

Fig. 3. Signal flow of the underwater robot control.

B. Experiment Parameters

In the experiment, the control sampling interval time is selected as 0.1s. The gains of the MIMO-ESO ISMC are designed as Table I.

Beside the proposed controller, we have also designed a PD controller for comparing the control performance, in which the velocity of the robot are calculated by the direct deriviations of the position information. The parameters of the PD control are designed as $K_{\bar{p}} = \mathrm{diag}[180, 50, 40, 0.2, 0.2, 3]$, and $K_{\bar{d}} = \mathrm{diag}[10, 10, 10, 2, 2, 2]$. The initial position and orientation of the underwater robot are set as $\eta_0 = [1.4m, 1.8m, 0.6m, 0rad, 0rad, -\frac{\pi}{4}rad]^\top$. Note that in different experiments, there will be a slight variation of the initial states due to the the deployment error. The nominal hydrodynamic parameters G_η, M^*, D^*, C^* and L in the designed control are $G_\eta = 0_{6\times6}$, $M^* = \mathrm{diag}[121.8, 127, 134.1, 32.62, 33.87, 33.87]$, $D^* = \mathrm{diag}[13 +$

TABLE I
CONTROL GAINS OF THE MIMO-ESO ISMC.

Gain	Value
γ_1	1
γ_2	1.5
c_1	0.8
w_0	1.5
K_p	diag[0.55, 1.2, 1.5, 0.5, 0.8, 0.06]
K_i	diag[3, 0.8, 0.8, 0.6, 0.4, 0.8]
K_d	diag[0.1, 0.1, 0.1, 0.1, 0.1, 0.1]
K_{sw}	diag[0.003, 0.0024, 0.002, 0.0025, 0.003, 0.0026]
K_s	diag[0.3, 0.3, 0.3, 0.3, 0.3, 0.3]

$50|u|, 14.3 + 50.2|v|, 21.2 + 64.7|w|, 18 + 73.8|p|, 24.3 + 101.7|q|, 19.2 + 84.1|r|]$,

$$C^* = \begin{bmatrix} 0 & 0 & 0 & 0 & 134.1w & -127v \\ 0 & 0 & 0 & -134.1w & 0 & 121.8u \\ 0 & 0 & 0 & 127v & -121.8u & 0 \\ 0 & 134.1w & -127v & 0 & 33.87r & -33.87q \\ -134.1w & 0 & 121.8u & -33.87r & 0 & 32.62p \\ -127v & -121.8u & 0 & 33.87q & -32.62p & 0 \end{bmatrix}$$

$$L = \begin{bmatrix} 1 & 0 & 0 & 0 & 1 & 0 \\ 0 & 1 & 0 & 1 & 0 & 0 \\ 0 & 0 & 1 & 0 & 0 & 0 \\ 0 & 0 & 0.287 & 0 & 0 & -0.287 \\ 0.277 & 0 & 0 & 0 & -0.277 & 0 \\ 0 & 0.287 & 0 & -0.287 & 0 & 0 \end{bmatrix}$$

The $h_1(t)$ is selected as $h_1(t) = 1/(t+1)$ and the desired trajectory is $x_r(t) = 0.6\sin(t/20) + 1.2$, $y_r(t) = 0.4\cos(t/20) + 1.2$, and $z_r(t) = 0.0025t + 0.5$.

C. Experiment Results With Robust Test

To justify the controller performance against external disturbances, robustness tests have been done for the PD and the proposed controller in the experiment. At $t = 87s$, there is an instantaneous external force, which lasts for $0.2s$, acting on the robot during the experiment.

The trajectory tracking results of the experiment in the 3D space and in the horizontal plane are presented in Fig. 4. Intuitively, both the PD controller and the proposed controller are able to steer the robot following the desired trajectory. To compare the two controllers, we define the RMS value of the tracking error as $\|e\|_{RMS} = \sqrt{\frac{1}{N}\sum_{i=1}^{N}\|e(i)\|^2}$, where N is the total sampling numbers in the experiment. The RMS values for both controllers is shown in Table II.

Fig. 5 takes further analysis of the tracking result and it shows the trajectory tracking errors of the underwater robot in each channel. Note that, from Fig. 5(a)-Fig. 5(f) and Table II, the tracking error with PD controller in each channel is greater error than the proposed one. Moreover, after the disturbance at 87s as mentioned above, the proposed controller shows less overshooting and needs less time to recover, compared with the PD controller. Fig. 6 presents the control inputs of the six thrusts, under the PD and proposed controller. Fig. 7 illustrates the output of the disturbance estimation in experiment.

To validate the performance of the ESO clearly, we provide simulation results in Fig. 8. In the simulation, the controller and the parameters are chosen as the same as that used in the experiment. To imitate the measurement noise of VPS and IMU, we add the white noise with standard deviations $0.05m$ and $0.05rad$ for position and angular measurement, respectively. The hydrodynamic parameters in the robot are selected as the nominal value with 10% uncertainties added. To verify the robustness performance, at $t = 87s$, there is an instantaneous external force, which lasts for $3s$, acting on the robot during the simulation. Fig. 8 shows that the ESO can estimate the external disturbance.

Comparison of the experimental results indicates that no matter in the presence or absence of the disturbance, the proposed controller tracks the desired trajectory more precisely with less tracking deviation than the conventional PD controller. Although the proposed controller has large control inputs and fluctuations during the course as shown in Fig. 6. The robustness test shows that the proposed controller is better than PD controller in terms of peak overshoots and convergence rates.

TABLE II
RMS ERROR OF PD CONTROLLER AND MIMO-ISMC.

$\|e\|_{RMS}$	PD	MIMO-ESO ISMC
X(m)	0.0438	0.0209
Y(m)	0.0539	0.0294
Z(m)	0.037	0.0143
$\phi(^\circ)$	5.92	1.59
$\theta(^\circ)$	8.04	2.52
$\psi(^\circ)$	5.48	2.27

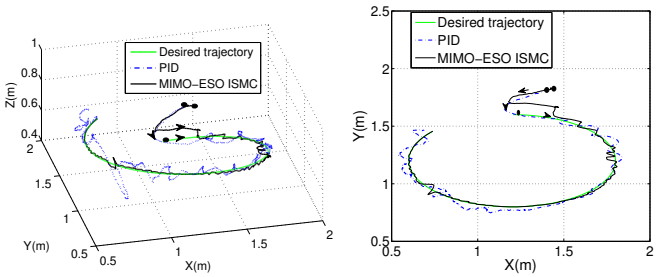

(a) (b)

Fig. 4. (a) Trajectory in 3D space. (b) Trajectory in the horizontal plane.

Note that there are some aspects that may have influences on the experimental results; (i) the underwater robot used in the experiment has six low cost thrusters with different characteristics, such as respond time, size of dead-zone, which degrades the control performance of the robot especially in case that the calculated control input is small. (ii) The performance of the PD control could be improved if we carefully adjust the control parameters and add the integral items. However, this is empirical and will take more time to achieve a better performance. (iii) Chattering phenomenon still exists in the experiment because the switching control is applied. To reduce chattering, the saturation function can be employed to replace the sgn function. However, this may reduce the robustness of the controller against the uncertainties and disturbances.

VI. CONCLUSION

In this paper, a novel integral sliding mode control based on an adaptive MIMO-ESO has been developed for a general type of underwater robots. Asymptotic convergence of both tracking error and estimation error were achieved even in presence of unknown external disturbances and model

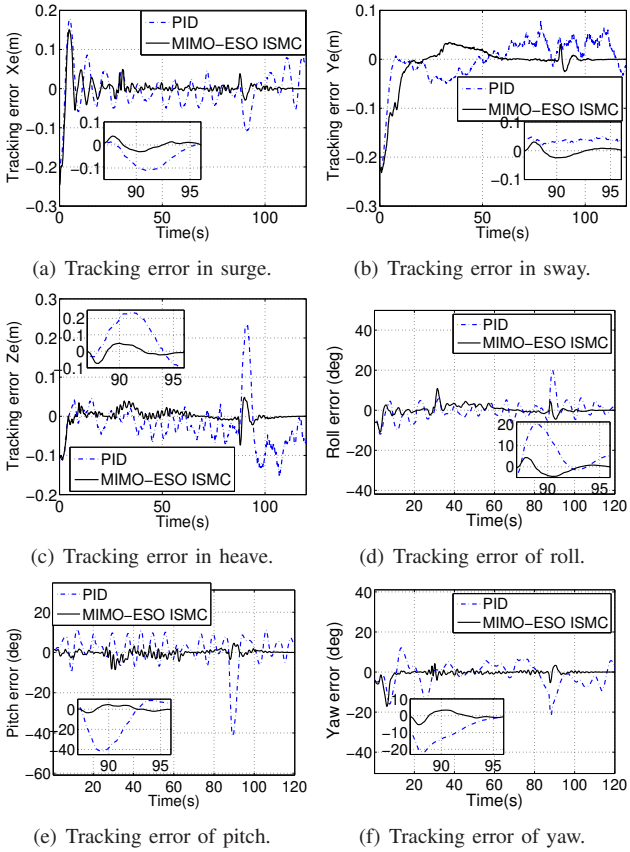

(a) Tracking error in surge. (b) Tracking error in sway.

(c) Tracking error in heave. (d) Tracking error of roll.

(e) Tracking error of pitch. (f) Tracking error of yaw.

Fig. 5. Trajectory tracking errors in the experiment.

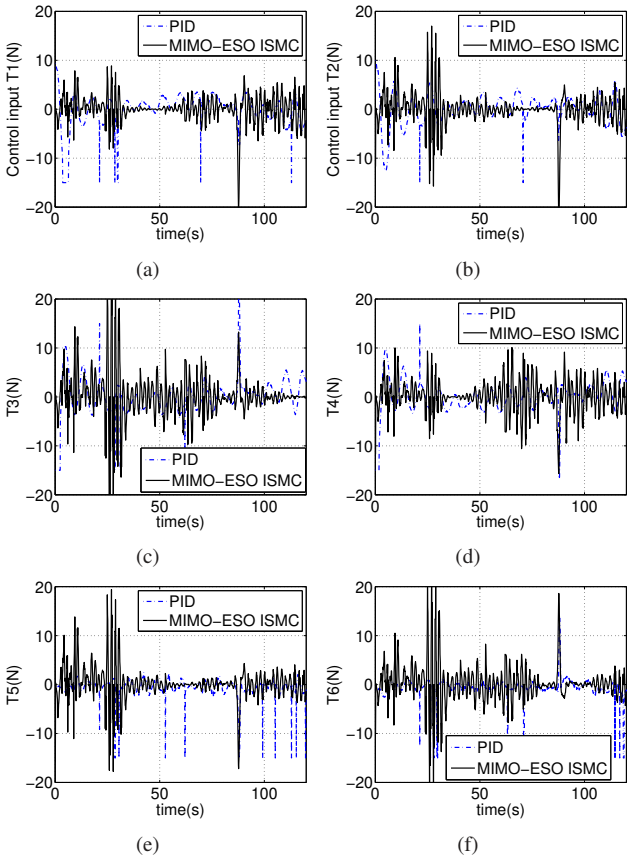

(a) (b)

(c) (d)

(e) (f)

Fig. 6. Control inputs of the controllers.

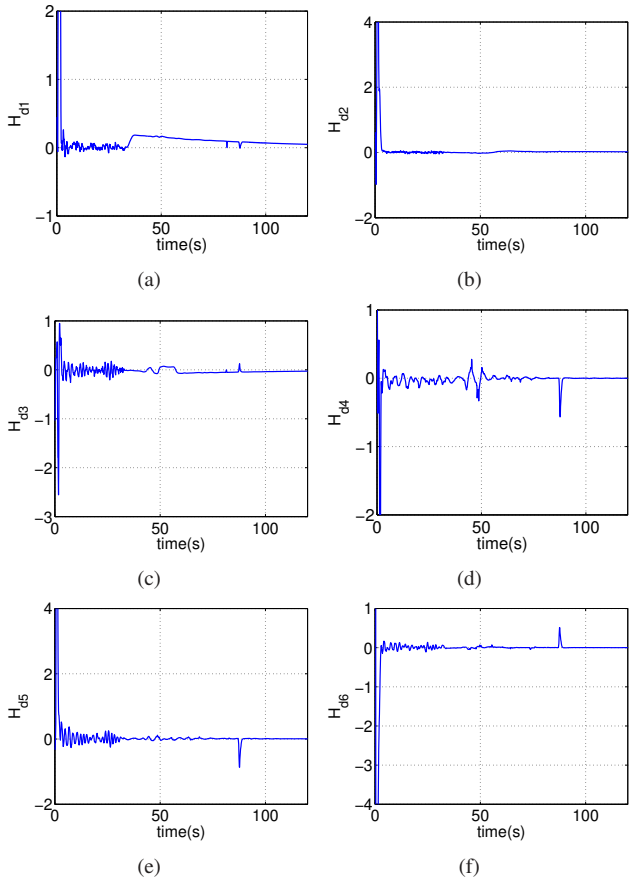

(a) (b)

(c) (d)

(e) (f)

Fig. 7. Estimation of disturbances in the experiment.

uncertainties. Comparative experimental studies verified the effectiveness and illustrate the supervior performance of the proposed control.

REFERENCES

[1] Z. Li, C. Yang, N. Ding, S. Bogdan, and T. Ge, "Robust adaptive motion control for underwater remotely operated vehicles with velocity constraints," *International Journal of Control, Automation & Systems*, vol. 10, no. 2, pp. 421–429, 2012.

[2] W. He, Z. Yin, and C. Sun, "Adaptive neural network control of a marine vessel with constraints using the asymmetric barrier lyapunov function," *IEEE Transactions on Cybernetics*, 2016, doi:10.1109/TCYB.2016.2554621.

[3] Y. Shi, C. Shen, and B. Buckham, "Integrated path planning and tracking control of an AUV: A unified receding horizon optimization approach," *IEEE/ASME Transactions on Mechatronics*, 2016, doi:10.1109/TMECH.2016.2612689.

[4] H. Li, P. Xie, and W. Yan, "Receding horizon formation tracking control of constrained underactuated autonomous underwater vehicles," *IEEE Transactions on Industrial Electronics*, 2016, doi:10.1109/TIE.2016.2589921.

[5] Z. Chu, D. Zhu, and S. X. Yang, "Observer-based adaptive neural network trajectory tracking control for remotely operated vehicle," *IEEE Transactions on Neural Networks Learning Systems*, 2016, doi:10.1109/TNNLS.2016.2544786.

[6] C. S. Chin and S. H. Lum, "Rapid modeling and control systems prototyping of a marine robotic vehicle with model uncertainties using xPC Target system," *Ocean Engineering*, vol. 38, no. 17-18, pp. 2128–2141, Dec 2011.

[7] B. Miao, T. Li, and W. Luo, "A DSC and MLP based robust adaptive NN tracking control for underwater vehicle," *Neurocomputing*, vol. 111, no. 6, pp. 184–189, 2013.

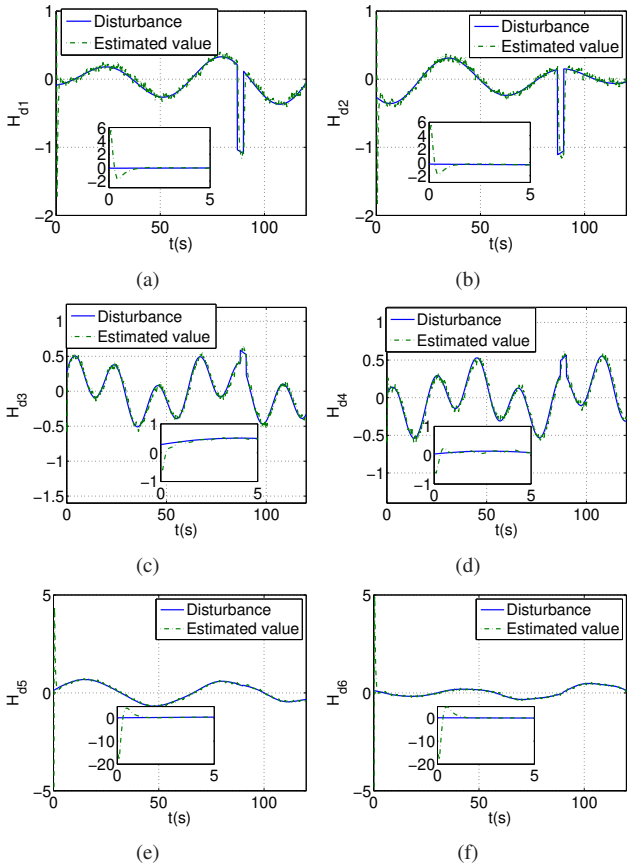

Fig. 8. Estimation of disturbances in the simulation.

[8] A. Bagheri, T. Karimi, and N. Amanifard, "Tracking performance control of a cable communicated underwater vehicle using adaptive neural network controllers," *Applied Soft Computing*, vol. 10, no. 3, pp. 908–918, 2010.

[9] H. Ashrafiuon, K. R. Muske, L. C. Mcninch, and R. A. Soltan, "Sliding-mode tracking control of surface vessels," *IEEE Transactions on Industrial Electronics*, vol. 55, no. 11, pp. 4004–4012, 2008.

[10] H. Joe, "Integral sliding mode controller for precise maneuvering of autonomous underwater vehicle in the presence of unknown environmental disturbances," *International Journal of Control*, vol. 88, no. 10, pp. 1–43, 2015.

[11] C. E. Hall and Y. B. Shtessel, "Sliding mode disturbance observer-based control for a reusable launch vehicle," *Journal of Guidance Control & Dynamics*, vol. 29, no. 6, pp. 1315–1328, 2006.

[12] Q. Guo, Y. Zhang, B. Celler, and S. Su, "Backstepping control of electro-hydraulic systems based on extended-state-observer with plant dynamics largely unknown," *IEEE Transactions on Industrial Electronics*, vol. 63, no. 11, pp. 6909–6921, 2016.

[13] C. Yang, X. Wang, L. Cheng, and H. Ma, "Neural-learning-based telerobot control with guaranteed performance," *IEEE Transactions on Cybernetics*, 2016, doi:10.1109/TCYB.2016.2573837.

[14] E. Sebasti and M. A. Sotelo, "Adaptive fuzzy sliding mode controller for the kinematic variables of an underwater vehicle," *Journal of Intelligent & Robotic Systems*, vol. 49, no. 2, pp. 189–215, 2007.

[15] Z. Peng, D. Wang, Y. Shi, H. Wang, and W. Wang, "Containment control of networked autonomous underwater vehicles with model uncertainty and ocean disturbances guided by multiple leaders," *Information Sciences*, vol. 316, pp. 163–179, 2015.

[16] L. Wu, W. X. Zheng, and H. Gao, "Dissipativity-based sliding mode control of switched stochastic systems," *IEEE Transactions on Automatic Control*, vol. 58, no. 3, pp. 785–791, March 2013.

[17] S. Li, X. Wang, and L. Zhang, "Finite-time output feedback tracking control for autonomous underwater vehicles," *IEEE Journal of Oceanic Engineering*, vol. 40, no. 3, pp. 727–751, July 2015.

[18] H. Li, P. Shi, and D. Yao, "Adaptive sliding mode control of markov jump nonlinear systems with actuator faults," *IEEE Transactions on Automatic Control*, 2016, doi:10.1109/TAC.2016.2588885.

[19] C. S. Chin and C. Wheeler, "Sliding-mode control of an electromagnetic actuated conveyance system using contactless sensing," *IEEE Transactions on Industrial Electronics*, vol. 60, no. 11, pp. 5315–5324, Nov 2013.

[20] L. Wu, Z. Feng, and J. Lam, "Stability and synchronization of discrete-time neural networks with switching parameters and time-varying delays," *IEEE Transactions on Neural Networks and Learning Systems*, vol. 24, no. 12, pp. 1957–1972, Dec 2013.

[21] J. Liu, S. Vazquez, L. Wu, A. Marquez, H. Gao, and L. G. Franquelo, "Extended state observer based sliding mode control for three-phase power converters," *IEEE Transactions on Industrial Electronics*, vol. 64, no. 1, pp. 22–31, 2017.

[22] J. Kim, H. Joe, S. C. Yu, and J. S. Lee, "Time delay controller design for position control of autonomous underwater vehicle under disturbances," *IEEE Transactions on Industrial Electronics*, vol. 63, no. 2, pp. 1052–1061, 2016.

[23] H. Joe, M. Kim, and S. C. Yu, "Second-order sliding-mode controller for autonomous underwater vehicle in the presence of unknown disturbances," *Nonlinear Dynamics*, vol. 78, no. 1, pp. 183–196, 2014.

[24] E. Zheng, J. Xiong, and J. Luo, "Second order sliding mode control for a quadrotor uav," *ISA transactions*, vol. 53, no. 4, pp. 1350–1356, 2014.

[25] S. Soylu, B. J. Buckham, and R. P. Podhorodeski, "A chattering-free sliding-mode controller for underwater vehicles with fault-tolerant infinity-norm thrust allocation," *Ocean Engineering*, vol. 35, no. 16, pp. 1647–1659, 2008.

[26] D. Ginoya, P. D. Shendge, and S. B. Phadke, "Sliding mode control for mismatched uncertain systems using an extended disturbance observer," *IEEE Transactions on Industrial Electronics*, vol. 61, no. 4, pp. 1983–1992, 2014.

[27] T. Elmokadem, M. Zribi, and K. Youcef-Toumi, "Terminal sliding mode control for the trajectory tracking of underactuated autonomous underwater vehicles," *Ocean Engineering*, vol. 129, pp. 613–625, 2017.

[28] J. Na, X. Ren, and D. Zheng, "Adaptive control for nonlinear pure-feedback systems with high-order sliding mode observer," *IEEE Transactions on Neural Networks and Learning Systems*, vol. 24, no. 3, pp. 370–382, 2013.

[29] D. Fernandes, A. J. Sorensen, K. Y. Pettersen, and D. C. Donha, "Output feedback motion control system for observation class ROVs based on a high-gain state observer: Theoretical and experimental results," *Control Engineering Practice*, vol. 39, pp. 90–102, 2015.

[30] H. An, J. Liu, C. Wang, and L. Wu, "Disturbance observer-based antiwindup control for air-breathing hypersonic vehicles," *IEEE Transactions on Industrial Electronics*, vol. 63, no. 5, pp. 3038–3049, 2016.

[31] J. Yao, Z. Jiao, and D. Ma, "Extended-state-observer-based output feedback nonlinear robust control of hydraulic systems with backstepping," *IEEE Transactions on Industrial Electronics*, vol. 61, no. 61, pp. 6285–6293, 2014.

[32] L. Wu, X. Su, and P. Shi, "Output feedback control of markovian jump repeated scalar nonlinear systems," *IEEE Transactions on Automatic Control*, vol. 59, no. 1, pp. 199–204, 2014.

[33] G. Xia, C. Pang, and J. Liu, "Neural-network-based adaptive observer design for autonomous underwater vehicle in shallow water," in *International Conference on Natural Computation*, 2013, pp. 216–221.

[34] Z. Chu and M. Zhang, "Fault reconstruction of thruster for autonomous underwater vehicle based on terminal sliding mode observer," *Ocean Engineering*, vol. 88, no. 5, pp. 426–434, 2014.

[35] Z. Li, C. Y. Su, G. Li, and H. Su, "Fuzzy approximation-based adaptive backstepping control of an exoskeleton for human upper limbs," *IEEE Transactions on Fuzzy Systems*, vol. 23, no. 3, pp. 555–566, June 2015.

[36] B. Xian, D. Chen, B. Zhao, and Y. Zhang, "Nonlinear robust output feedback tracking control of a quadrotor uav using quaternion representation," *Nonlinear Dynamics*, vol. 79, no. 4, pp. 2735–2752, 2015.

[37] H. Castañeda, S. O. Salas-Peña, and J. León-Morales, "Extended observer based on adaptive second order sliding mode control for a fixed wing UAV," *ISA Transactions*, 2016.

[38] W. Kim, D. Won, D. Shin, and C. C. Chung, "Output feedback nonlinear control for electro-hydraulic systems," *Mechatronics*, vol. 22, no. 6, pp. 766–777, 2012.

[39] T. I. Fossen, *Guidance and Control of Ocean Vehicles*. New York: Wiley Interscience, 1994.

[40] A. Azemi and E. E. Yaz, "Sliding-mode adaptive observer approach to chaotic synchronization," *Journal of Dynamic Systems Measurement & Control*, vol. 122, no. 4, pp. 758–765, 2000.

[41] B. Walcott and S. Zak, "State observation of nonlinear uncertain dynamical systems," *IEEE Transactions on Automatic Control*, vol. 32, no. 2, pp. 166–170, 1987.
[42] K. Kalsi, J. Lian, and S. Hui, "Sliding-mode observers for systems with unknown inputs: A high-gain approach," *Automatica*, vol. 46, no. 2, pp. 347–353, 2010.
[43] Y. Li and Q. Xu, "Adaptive sliding mode control with perturbation estimation and pid sliding surface for motion tracking of a piezo-driven micromanipulator," *IEEE Transactions on Control Systems Technology*, vol. 18, no. 4, pp. 798–810, 2010.
[44] I. Eker, "Sliding mode control with pid sliding surface and experimental application to an electromechanical plant," *ISA transactions*, vol. 45, no. 1, pp. 109–118, 2006.
[45] G. Tao, "A simple alternative to the barbalat lemma," *IEEE Transactions on Automatic Control*, vol. 42, no. 5, p. 698, 1997.

Rongxin Cui (M'09) received B.Eng. and Ph.D. degrees from Northwestern Polytechnical University, Xi'an, China, in 2003 and 2008, respectively. From August 2008 to August 2010, he worked as a Research Fellow at the Centre for Offshore Research & Engineering, National University of Singapore, Singapore. Currently, he is a Professor with the School of Marine Science and Technology, Northwestern Polytechnical University, Xi'an, China. His current research interests are control of nonlinear systems, cooperative path planning and control for multiple robots, control and navigation for underwater vehicles, and system development.

Dr. Cui servers as an Editor for the Journal of Intelligent & Robotic Systems.

PLACE PHOTO HERE

Lepeng Chen received B.Eng. degree from Northwestern Polytechnical University, Xi'an, China, in 2015.

He is currently pursuing the Ph.D. degree at the School of Marine Science and Technology, Northwestern Polytechnical University, Xi'an, China. His research interests are adaptive control and its applications to marine vehicles.

Chenguang Yang (M'10-SM'16) received the B.Eng. degree in measurement and control from Northwestern Polytechnical University, Xi'an, China, in 2005, and the Ph.D. degree in control engineering from the National University of Singapore, Singapore, in 2010. He received postdoctoral training at Imperial College London, UK. He is a senior lecturer with Zienkiewicz Centre for Computational Engineering, Swansea University, UK. His research interests lie in robotics, automation and computational intelligence.

Mou Chen (M'10) received the B.S. degree in material science and engineering and the Ph.D. degree in control theory and control engineering from Nanjing University of Aeronautics and Astronautics (NUAA), Nanjing, China, in 1998 and 2004, respectively. He is currently a full Professor in the College of Automation Engineering, NUAA. He was an Academic Visitor in the Department of Aeronautical and Automotive Engineering, Loughborough University, Loughborough, U.K., from November 2007 to February 2008. From June 2008 to September 2009, he was a Research Fellow in the Department of Electrical and Computer Engineering, National University of Singapore. He was a Senior Academic Visitor in the School of Electrical and Electronic Engineering, University of Adelaide, Adelaide, Australia, from May 2014 to November 2014. His research interests include nonlinear system control, intelligent control, and flight control.